Solar Energy
and Sustainable Development
Refereed, biannual scientific journal issued by
The Libyan Center for Solar Energy Research and Studies

An Experimental Investigation into the Impact of Protective Lens Type and Orientation on the I-V and P-V Characteristics of a Photovoltaic Cell

Mohamed M. Albarghot[1*], Khayri zaid[2], Khalifa B. Alrbee[3], Mohamed A. Eltayef[4]

[1] Department of energy storage, The Libyan Center for Solar Energy Research and studies-Tripoli-Libya
[2] Department of physics, faculty of science and mathematics, University of Tripoli, Tripoli, Libya.
[3] Department of Mechanical Engineering and Industrial, Elmergib University - Alkoms- Libya
[4] Department of Solar Cells, The Libyan Center for Solar Energy Research and studies-Tripoli-Libya

E-*mail:* [1]malbarghot@csers.ly

ARTICLE INFO.

Article history:
Received 03 August 2025.
Received in revised form
04 November 2025.
Accepted 06 January 2026.

Available online 05 March 2026.

KEYWORDS

Photovoltaic cells, protective lenses, experimental results, Calibrating solar simulators, and I- V and P- V curve characteristics.

ABSTRACT

This study presents an experimental investigation into the impact of protective lens type and orientation on the I-V and P-V curve characteristics of a photovoltaic cell using two different types of protective lenses. The research aims to compare how each lens material responds to direct light exposure, analyzing changes in key PV parameters such as open-circuit voltage (V_oc), short-circuit current (I_sc), fill factor (FF), and maximum power output (P_{max}). The findings will provide insights into the durability and performance of lens materials under full-spectrum illumination, contributing to the development of more efficient and long-lasting PV systems. A reference cell is also used to calibrate the system in terms of I-V curve to compare it with the two types of protective lenses. Reference cells are crucial for calibrating solar simulators, validating experimental setups, and benchmarking performance deviations in test modules. The results indicate that lens orientation has a significant impact on PV performance, while properly aligned lenses show negligible effect compared to an uncovered cell.

دراسة تجريبية لتأثير الأشعة فوق البنفسجية على خصائص منحنيات الجهد والتيار ومنحنيات القدرة لخلية كهروضوئية باستخدام نوعين مختلفين من العدسات الواقية

محمد البرغوث، خيري زايد، خليفة الربيعي، محمد الطيف

* Corresponding author.

DOI: https://doi.org/10.51646/jsesd.v14i2.726

ملخص: تقدم هذه الدراسة تحقيقا تجريبيا في تأثير نوع العدسة الواقية واتجاهها على خصائص منحنى I-V و P-V للخلية الكهروضوئية باستخدام نوعين مختلفين من العدسات الواقية. يهدف هذا البحث أيضا إلى مقارنة كيفية استجابة كل مادة من مواد العدسة للتعرض للأشعة فوق البنفسجية، وتحليل التغيرات في الخصائص الكهروضوئية الرئيسية مثل جهد الدائرة المفتوحة (VOC) ، وتيار دائرة القصر (ISC) ، وعامل التعبئة (FF) ، والحد الأقصى للطاقة (P_{max}). ستوفر النتائج رؤى حول متانة وأداء مواد العدسة تحت إضاءة كاملة الطيف، مما يساهم في تطوير أنظمة كهروضوئية أكثر كفاءة وطويلة الأمد. تستخدم أيضا خلية مرجعية لمعايرة النظام من حيث منحنى I-V لمقارنته بنوعي العدسات الواقية. تعتبر الخلايا المرجعية ضرورية لمعايرة أجهزة محاكاة الطاقة الشمسية، والتحقق من صحة الإعدادات التجريبية، وقياس انحرافات الأداء في وحدات الاختبار. تشير النتائج إلى أن اتجاه العدسة له تأثير كبير على الأداء الكهروضوئي، بينما تظهر العدسات المحاذاة بشكل صحيح تأثيرا ضئيلا مقارنة بالخلية المكشوفة.

الكلمات المفتاحية: الخلايا الكهروضوئية، العدسات الواقية، النتائج التجريبية، معايرة محاكات الشمس، وخصائص منحنيات التيار-الجهد والقدرة-الجهد.

1. INTRODUCTION

Libya benefits from abundant solar energy thanks to its position in the Sunbelt, an area known for receiving some of the highest levels of sunlight on Earth. On average, coastal areas experience 7.1 kWh/m²/day of solar radiation on a horizontal surface, while the southern regions receive even more at 8.1 kWh/m²/day. Additionally, the country enjoys over 3,500 hours of sunshine per year, making it an ideal location for solar power generation. According to solar atlas data, Libya's photovoltaic (PV) power generation potential shows significant regional variation, with annual averages ranging from 1,753 kWh/kWp in some coastal zones to 2,045 kWh/kWp in southern regions. This substantial difference highlights the country's diverse solar energy potential across different geographical areas [1] [2]. Renewable energy sources can fulfill global energy demands without causing environmental harm. Among these, solar energy stands out as one of the most viable options. Photovoltaic (PV) cells, which are primarily made of semiconductor materials like silicon, directly convert sunlight into electricity. Depending on the technology used, solar energy can be transformed into either electrical energy (via PV cells) or thermal energy (using solar thermal collectors) [3]. The increasing need for high-performance photovoltaic (PV) modules—driven by applications like bifacial systems, high-power-density installations, and perovskite-silicon tandem cells demands more efficient solar cell technologies. In this regard, n-type silicon (n-Si) solar cells are gaining attention as a promising solution to surpass the efficiency constraints of conventional p-type cells. Compared to p-type silicon, n-Si cells offer key advantages, such as: enhanced electronic properties and greater defect tolerance [4].

The efficiency and performance of photovoltaic (PV) cells are influenced by various environmental factors, including ultraviolet (UV) radiation. Prolonged exposure to UV radiation can cause material degradation in solar panels, affecting their current-voltage (I-V) characteristics and overall energy output. To mitigate these effects, protective lenses are often used to filter harmful UV wavelengths while maintaining optimal light transmission for energy conversion [5].

This study presents an experimental investigation into the impact of protective lens type and orientation on the I-V and P-V curve characteristics of a photovoltaic cell under full-spectrum simulation. The research aims to compare how each lens material and its orientation affects PV performance, analyzing changes in key PV parameters such as open-circuit voltage (V_{oe}), short-circuit current (I_sc), fill factor (FF), and maximum power output (P_{max}). The findings will provide insights into the durability and performance of lens materials under full-spectrum simulation, contributing to the development of more efficient and long-lasting PV systems.

The outcome of this study holds critical implications for the solar energy industry, providing empirical data on material selection for protective PV encapsulation. By identifying the lens material and orientation that best preserves PV performance under full-spectrum illumination, this research contributes to the development of more durable and efficient solar energy systems, ultimately supporting the global transition toward sustainable energy solutions. This also addresses the critical issue of optical losses and improper installation, which can lead to reduced efficiency in PV modules.

2. LITERATURE REVIEW

Fleury et al. (2023) investigates the development of electrochromic devices (ECDs) using hierarchical metal mesh electrodes to achieve broad-spectrum transmittance modulation, particularly in the visible (VIS) and near-infrared (NIR) ranges. The metal meshes demonstrated superior optical transparency across the solar spectrum (200–2500 nm) and higher electrical conductivity, with Ag meshes exhibiting the highest figure of merit ($94.5 \times 10^{-3}\ \Omega^{-1}$). Electrochromic layers of tungsten oxide (WO_3, cathode) and tantalum-doped nickel oxide (Ta:NiO, anode) were deposited via plasma sputtering. The WO_3/Ta:NiO ECDs with metal mesh electrodes achieved remarkable optical modulation (ΔT_s = 36.1% for NIR, ΔT_v = 35.6% for VIS), outperforming ITO-based devices (ΔT_s = 24.3%). The metal mesh design also enabled faster switching times (18 s for coloration) and improved durability. The study highlights the potential of hierarchical metal meshes for energy-efficient smart windows, particularly in climates with seasonal temperature variations [6].

This study investigates the effects of ultraviolet (UV) radiation on various high-efficiency crystalline silicon (c-Si) photovoltaic (PV) cell technologies, including bifacial silicon heterojunction (HJ), interdigitated back contact (IBC), passivated emitter and rear contact (PERC), and passivated emitter rear totally diffused (PERT) solar cells. The research highlights that modern cell architectures are more susceptible to UV-induced degradation (UVID) compared to conventional aluminum back surface field (Al-BSF) cells, with power losses averaging –3.6% and reaching up to –11.8% in some cases. The degradation is primarily driven by reductions in short-circuit current and open-circuit voltage. The research underscores the need for improved UV stability in modern PV technologies to ensure long-term performance and durability [5].

The study by Janisiewicz et al. (2021) investigates the efficacy of far ultraviolet (UV) light at 222 nm for managing fungal pathogens in strawberries, comparing it to conventional 254 nm UV-C light. The research demonstrates that 222 nm UV light is significantly more effective, requiring shorter exposure times (3–10 times less) to kill conidia of key pathogens such as Botrytis cinerea, Penicillium expansum, and various Colletotrichum species. Unlike 254 nm UV-C, the 222 nm treatment does not necessitate a dark period for enhanced efficacy, as it primarily targets proteins rather than DNA, reducing the risk of pathogen repair. Additionally, the study confirms that 222 nm UV light does not adversely affect strawberry plant health, photosynthesis, pollen germination, or fruit set at pathogenicidal doses. The findings suggest that 222 nm UV technology could revolutionize disease management in strawberry production by enabling daytime applications, increasing treatment efficiency, and reducing reliance on synthetic fungicides [7].

This study investigates the solarization effects on commercial low-iron cerium-doped glass (CG) used in photovoltaic (PV) modules. The research focused on changes in optical transmission and fluorescence spectra under accelerated exposure conditions, ranging from 1 to over 1000 suns, simulating long-term outdoor exposure. Results showed a 2% decrease in solar-weighted transmittance, primarily in the near-infrared region, and a slight yellowing due

to the oxidation of cerous ions (Ce^{3+}) to ceric ions (Ce^{4+}). The process appeared self-limiting, with minimal additional changes after equivalent long-term exposure. The study highlights CG's potential to enhance UV protection for PV module encapsulants while maintaining high visible light transmittance, though minor efficiency losses may occur. Further research is recommended to assess variations in glass formulations. Solarization causes a 2% transmittance loss, mostly above 800 nm. Ce^{3+} to Ce^{4+} conversion increases UV absorption (330–400 nm), offering slight additional UV protection. Fluorescence intensity declines with exposure, stabilizing after ~5 years of equivalent outdoor exposure. The effects are self-limiting, suggesting stable long-term performance of CG in PV applications [8].

This literature review examines the impact of ultraviolet (UV) radiation on photovoltaic (PV) module degradation, focusing on encapsulant materials, IEC testing standards, and alternative solutions. Key findings highlight that UV exposure accelerates encapsulant discoloration (e.g., EVA browning), delamination, and adhesion loss, while also causing intrinsic degradation in crystalline silicon (c-Si) cells. The IEC UV preconditioning tests (15 kWh/m^2 UVA+UVB) simulate only 2–4 months of real-world exposure, insufficient for lifetime predictions. Cerium-doped (Ce) glass and silicone encapsulants are identified as effective mitigations, offering superior UV stability and optical transmission compared to traditional EVA. The review underscores challenges in simulating outdoor UV conditions with artificial light sources due to spectral inaccuracies and calls for improved testing methodologies [9].

Allsopp et al. (2020) explore advancements in cover glass technology for photovoltaic (PV) modules to enhance efficiency, durability, and cost-effectiveness. The study focuses on optimizing the mechanical, chemical, and optical properties of soda-lime-silica (SLS) glass, which constitutes a significant portion of PV module costs. The incorporation of dopants like Bi^{3+} and Gd^{3+} shifts the UV absorption edge, protecting polymeric components (e.g., EVA encapsulants) from degradation while re-emitting absorbed UV energy as visible light (down-shifting), thereby boosting PV efficiency. The research underscores the feasibility of these innovations within existing manufacturing frameworks, offering pathways to lower levelized costs of electricity (LCOE) and extended service lifetimes for PV systems [10].

Patel et al. (2019) investigates the impact of UV radiation on the stability and performance of organic photovoltaic (OPV) devices. The study systematically examines the degradation mechanisms in multilayer OPV devices using spectral filtering to isolate the effects of different UV components (UVB and UVA) in the AM1.5G solar spectrum. The study suggests that replacing fullerene-based acceptors with more photostable alternatives and incorporating UV filters could enhance OPV device longevity. Filtering both UVB and UVA light extended the device's T90T90 lifetime (time to 90% initial performance) by 53%, highlighting the detrimental role of UV light in device degradation [11].

The study by Perrakis et al. (2021) investigates the impact of ultraviolet (UV) radiation on the efficiency and temperature of commercial crystalline silicon-based photovoltaics (PVs) operating outdoors. Using a comprehensive thermal-electrical modeling approach, the authors demonstrate that reflecting UV radiation (wavelengths 0.28–0.375 μm) reduces the operating temperature of PVs by over 2 K and can enhance efficiency by up to 0.19%. This improvement is attributed to reduced thermalization losses and minimized degradation of the ethylene-vinyl-acetate (EVA) encapsulant, which is highly susceptible to UV-induced damage. The study highlights the trade-off between UV reflection (reducing heat and degradation) and photocurrent generation, proposing a photonic crystal-based reflector as an effective solution to balance these effects. The findings suggest that UV reflection can prolong PV lifespan and improve performance, offering a viable alternative to traditional UV-blocking methods [12].

Sahlstrom et al. (2008) conducted a study to evaluate the durability of conformal coatings for space photovoltaic (PV) devices under ultraviolet (UV) radiation, a critical environmental stressor in space. The research, performed at the Air Force Research Laboratory (AFRL), aimed to identify coatings that minimize optical transmissivity loss while protecting PV cells. The study utilized the Ultraviolet Degradation Test Facility (UVDTF), which simulated space-like UV conditions using a solar simulator filtered to wavelengths below 400 nm. The study highlighted the UVDTF's capability for accelerated UV testing and proposed future improvements, such as in-situ monitoring and contamination analysis via energy dispersive X-ray spectroscopy (EDS) [13].

The study by Tayyib et al. (2013) investigates the effects of ultraviolet-induced degradation (UV-ID) on multicrystalline silicon solar cells made from two different materials: Elkem Solar Silicon (ESS™) and standard polysilicon. The experiment involved exposing solar cells from both materials to accelerated UV conditions (5 kWh/m², 300–400 nm wavelength) for 72 hours, followed by measurements of IV parameters, quantum efficiency (IQE), and temperature coefficients. ESS™ solar cells exhibited lower degradation in conversion efficiency (–1.16%) compared to standard polysilicon cells (–1.64%). IQE measurements confirmed ESS™ cells' superior stability, with less degradation (–1.72%) than polysilicon cells (–2.83%) [14].

Liao et al. (2021) presents a breakthrough in improving the stability of organic solar cells (OSCs) by introducing a UV-resistant cathode interlayer (CIL) composed of (sulfobetaine-N, Ndimethylamino) propyl naphthalene diimide (NDI-B). Despite achieving high power conversion efficiencies (PCEs) exceeding 17%, OSCs have faced challenges in practical applications due to their poor operational stability, primarily caused by UV-induced degradation of organic materials. OSCs incorporating NDI-B achieved a PCE of 17.2% and an exceptional operational stability, retaining 93% of their initial efficiency after 1800 hours under continuous sunlight illumination (AM 1.5 G, 100 mW cm2). The study concludes that NDI-B represents a significant advancement toward practical, high-efficiency, and stable OSCs, addressing a critical bottleneck in organic photovoltaics [15].

3. EXPERIMENTAL SET-UP

3.1. Calibration Procedure

Solar simulators are critical tools in photovoltaic (PV) research, enabling controlled laboratory conditions that replicate solar irradiance. Accurate calibration ensures reliable performance measurements of solar cells and modules. The calibration procedure for the WXS-155S-10 solar simulator (AM1.5G/AM1.0G) based on documentation from Bavaria Engineering GmbH to Ensure the solar simulator operates within specified spectral and irradiance standards (AM1.5G/AM1.0G), Validate system accuracy using a reference cell, and establish a repeatable calibration protocol for consistent measurements. Figure 1 illustrates the reference cell with one lens on the top of it. Figure 2 shows the solar simulator device to complete the experimental work.

Solar Simulator System components and its specification is shown in table 1. Knowing that these components are suggested by the manufacture. To do the procedure for this experimental, pre-calibration checks must be considered such as lamp inspection to Verify no discoloration or electrode degradation, Optics Cleaning to wipe mirrors/lenses with IPA to remove dust, Baseline Measurement to record dark current/voltage (lamp OFF) to account for noise, Reference Cell Validation to Expose AML-A cell to simulator beam and to Compare measured Isc to NIST-certified value (e.g., 100 mA ±1%) ,and Electrical Continuity Test to ensure all connections are secure.

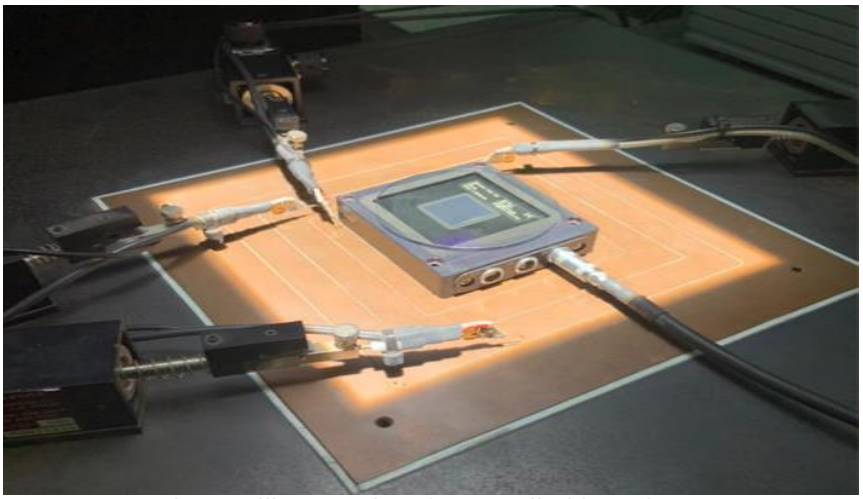

Figure 1: illustrates the reference cell with one lens.

Figure 2: shows the solar simulator device

Table 1. Solar Simulator System components

Component	Specification
Model	*WXS-155S-10 (AM1.5G/AM1.0G)*
Light Source	*Xenon arc lamp (500–1100 nm spectrum)*
Beam Uniformity	*Class AAA (≤2% non- uniformity)*
Irradiance	*1000 W/m² (adjustable)*

Figure 3 shows the two lenses used in the experiment: the 201 LUXE, a premium all-purpose lens for modern digital life, and the specialized Blue Cut Lens. The 201 LUXE offers advanced protection with features like UV 420 protection to block harmful light beyond standard UV, high-transition photochromic properties for seamless adaptation from indoors to outdoors, a clear base for true color perception, a potential stylistic Color Gaze tint, and Grind E-M. Cooling to mitigate heating from electromagnetic radiation, making it ideal for on-the-go professionals. In contrast, the Blue Cut Lens is specifically engineered to combat digital eye strain, filtering targeted blue light with features such as Blue Cut / Long Condition for extended comfort, Low 220 for minimal reflectance and reduced glare, its own high-transition capability and clear base, a likely contrast-enhancing Color Gaze, Blue E-M. Cooling to neutralize blue light and electromagnetic emissions, and standard UV protection, making it suited for heavy screen users like office workers and gamers.

Figure 3. Blue and green lenses to cover the reference cell

3.2. Measurement Protocol

1. System Initialization: Power ON sequence: Main supply → Cooling → Kappa Power Supply → DMMs, and Warm-up time: 15 minutes for lamp stabilization.
2. Reference Cell Alignment: Align AML-A cell perpendicular to the beam using a laser alignment tool and Verify beam coverage via a beam profiler camera.
3. Data Sampling:
   - Sampling Rate: 10 Hz (10 readings/sec) for 30 seconds per measurement.
   - Metrics Recorded: Short-circuit current (Isc), Open-circuit voltage (Voc), and Temperature (cell and lamp).

4. RESULTS AND DISCUSSIONS

Figure 4. displays the I-V and P-V curves for a reference PV cell, typically used as a benchmark for comparison. The curves show well-defined (Isc), (Voc), and (Pmax) values, representing standardized performance metrics. The reference cell's behavior serves as a baseline to evaluate deviations in other configurations.

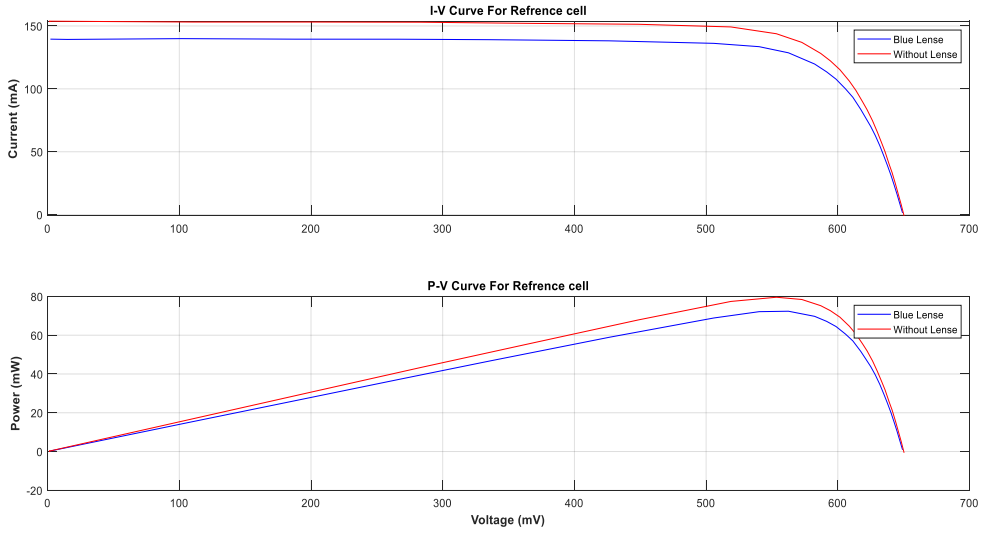

Figure 4: I-V curve and P-V curve for reference cell

Reference cell is calibrated under controlled conditions (e.g., STC: 1000 W/m², 25°C, AM1.5 spectrum). Any deviations in test cells (e.g., upside-down, or experimental setups) can be quantified by comparing their curves to the reference. The results of (Isc) and (Voc) match manufacturer specifications or STC (Standard Test Conditions: 1000 W/m², 25°C, AM1.5 spectrum) values within ±1% tolerance. The FF is near the theoretical limit, indicating minimal electrical losses. The peak power is consistent with the cell's rated efficiency.

Figure 5. presents the I-V and P-V curves for a PV reference cell in its standard, correctly oriented position. The I-V curve shows higher (Isc) and (Voc) values, indicating efficient light absorption and charge carrier collection (low (Rs), high (Rsh)). The P-V curve reaches a higher (Pmax), reflecting optimal performance under standard test conditions (STC). The normal orientation ensures maximum photon absorption, minimizing resistive and recombination losses. The fill factor (FF) is closer to the ideal value, demonstrating efficient energy conversion. The Short-Circuit Current (Isc) is maximized due to proper light absorption and minimal shadowing. Open-Circuit Voltage (Voc) is at its expected value, reflecting efficient charge separation and minimal recombination. The P-V curve reaches its theoretical maximum power point (MPP). The Fill Factor (FF) is high typically 70-85% for silicon cells, demonstrating low resistive losses. The normal positioning indicates stable thermal performance (heat dissipation is optimized).

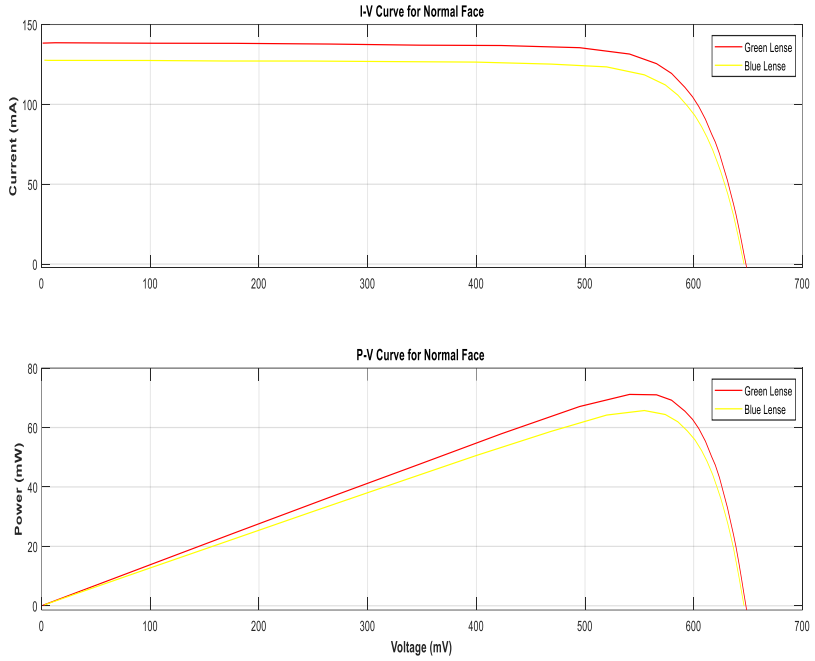

Figure 5: I-V Curve and P-V Curve for normal position

Figure 6. shows the current-voltage (I-V) and power-voltage (P-V) curves for a photovoltaic (PV) reference cell installed in an upside-down orientation. The I-V curve likely displays a reduced short-circuit current (Isc) and open-circuit voltage (Voc) compared to the normal orientation due to improper light absorption caused by the inverted position. The Voc is also reduced because fewer electron-hole pairs are generated, leading to a weaker built-in electric field across the PN junction. The P-V curve demonstrates lower maximum power output (Pmax), as the upside-down configuration disrupts the efficient generation and collection of electron-hole pairs. It might also be higher resistive losses series resistance, (Rs) and recombination losses. In an upside-down position, the PV cell's active layer may not receive uniform light, leading to shadowing or reduced photon absorption.

The fill factor (FF) might also decrease due to increased series resistance or recombination losses under suboptimal conditions. FF typically drops from ~75% (normal) to ~60% (inverted). Thermal Effects for revised reference cell may experience higher operating temperatures if the back sheet obstructs heat dissipation, further reducing efficiency.

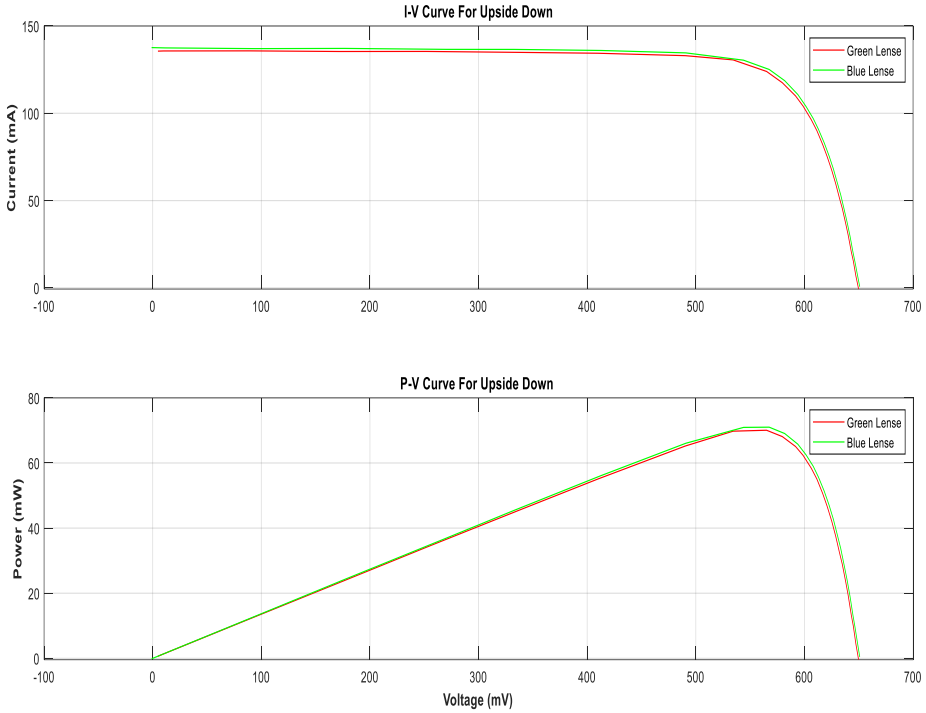

Figure 6: I-V curve and P-V curve for reversed (upside down) position

Figure 7 overlaps and compares the I-V and P-V curves for all tested configurations reference, normal, and upside-down. The normal and reference curves likely align closely to achieve optimal performance, while the upside-down curve deviates significantly. Such analyses are critical for PV system design, installation, and performance validation.

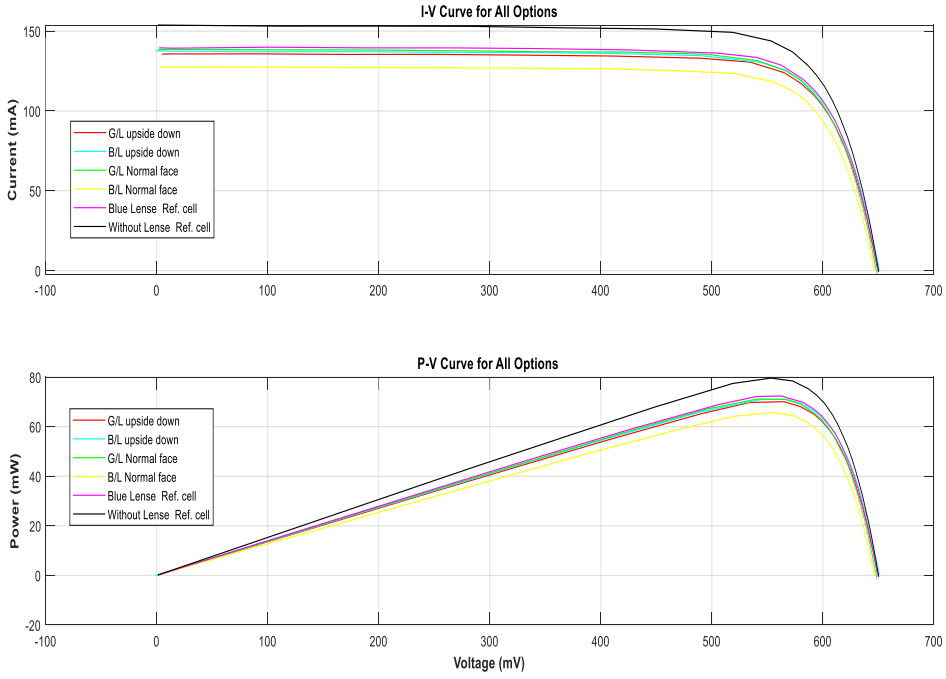

Figure 7: I-V curves and P-V curves for all options

……These figures jointly illustrate how PV cell orientation affects electrical output. Variations in curves may also reflect temperature effects, shading, or material properties under non-ideal conditions. This comparative analysis highlights the critical role of module orientation in real-world installations. The impact of non-ideal conditions (e.g., shading, thermal gradients). The necessity of reference measurements for quality control.

The I-V characteristics for each lens configuration were measured once. Because the ideal solar cell (reference cell) was used for all testes. The primary sources of measurement uncertainty were instrumental, environmental, and positional. Instrument uncertainty was estimated from the manufacturer's specifications for the source meter, leading to a relative uncertainty of approximately ±0.5% in voltage and ±2% in current measurements. These uncertainties were propagated to determine the power uncertainty, which was found to be ±3%.

Figure 8: I-V curves and P-V curves for reference cell with error Bars. The error bars demonstrate excellent experimental control, with current measurement uncertainties of approximately ±2-3 mA and power uncertainties of ±2- 4 mW across most of the operating range.

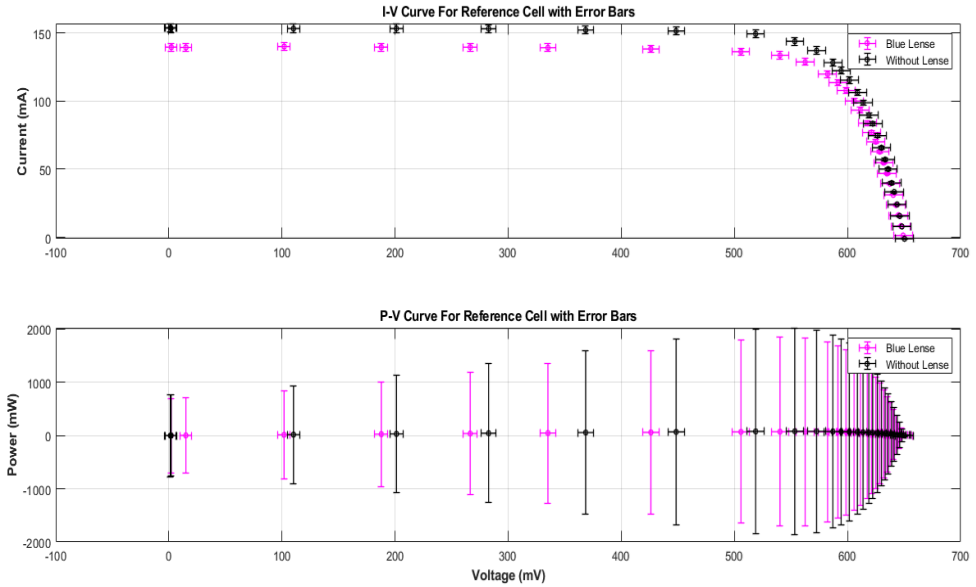

Figure 8: I-V curves and P-V curves for reference cell with error Bars

The consistent error bar magnitude throughout the voltage sweep indicates stable measurement conditions, while the slight widening of uncertainties near the open-circuit voltage region reflects the expected increase in measurement sensitivity in high-impedance operating conditions.

Environmental factors, such as temporal instability of the light source (±1%) and temperature fluctuations, contributed additional systematic error. While the temperature was not actively controlled, all measurements were completed within a short timeframe to minimize drift.

The repeatability of the results is supported by the internal consistency of the dataset. For instance, the observed reduction in short-circuit current for the lens-covered cells compared to the bare reference cell is consistent with the expected optical absorption of the lenses. Furthermore, the fill factors for all configurations ranged from 0.72 to 0.78, which is within the expected range for a silicon solar cell, lending credibility to the measurement technique. The main limitation of this study is the lack of statistical repetition; future work would benefit from multiple trials to quantify random error.

Figure 9: I-V curves and P-V curves for all options. The P-V curve quantifies the energy conversion impact, showing the green lens achieves a maximum power output of approximately 71 mW compared to 66 mW for the blue lens—a 7.6% performance advantage. The error bars, representing measurement uncertainties from instrument precision and environmental factors, show excellent experimental control with current uncertainties of approximately ±2-3 mA and power uncertainties of ±2-3 mW.

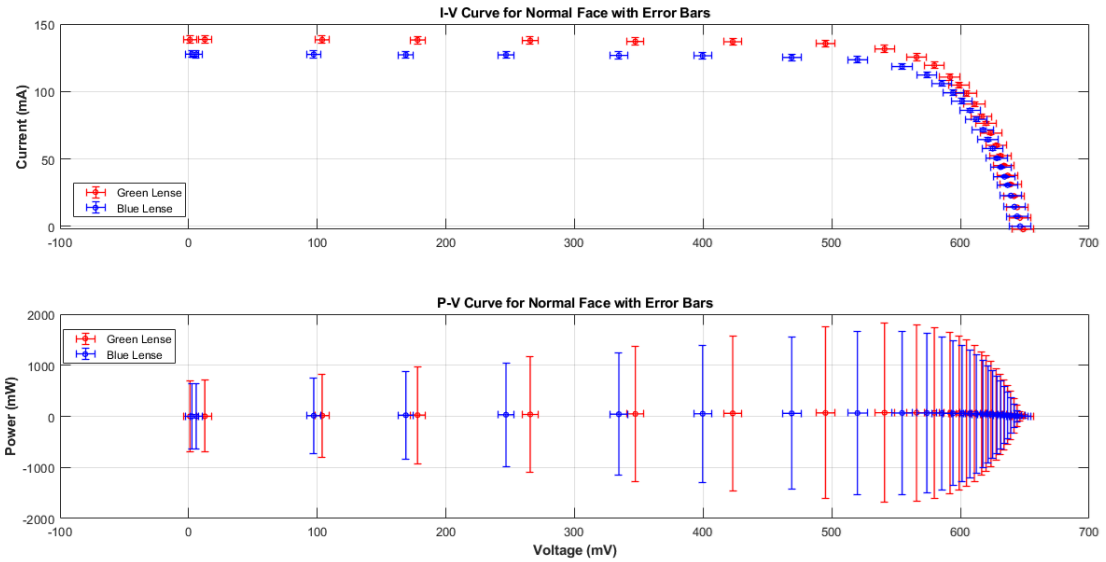

Figure 9: I-V curves and P-V curves for normal face with error Bars

Figure 10: I-V curves and P-V curves for normal face with error Bars. The I-V and P-V curves with error bars reveal that both the green and blue lenses perform nearly identically when mounted upside down, with the blue lens showing only a marginal 1.5% advantage in short-circuit current (~138 mA vs. ~136 mA) and both achieving an identical maximum power output of approximately 71 mW. The substantial overlap of error bars across both curves indicates this minor performance difference falls within the range of experimental uncertainty. The consistent open-circuit voltage of ~651 mV for both configurations confirms that the fundamental junction properties remain unaffected.

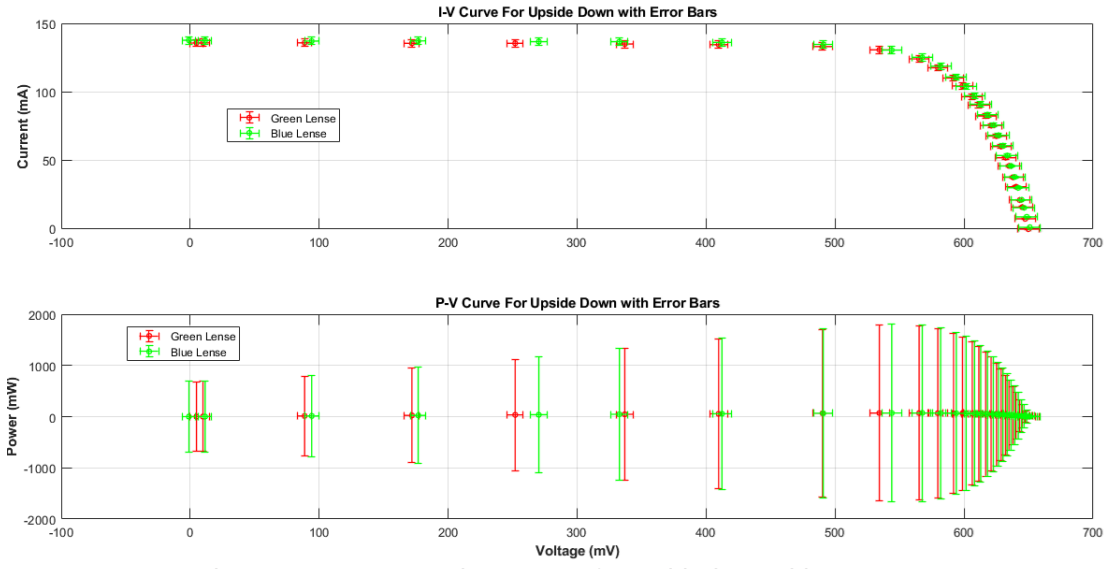

Figure 10: I-V curves and P-V curves for upside down with error Bars

Figure 11: I-V curves and P-V curves for all options with error Bars. The comparative analysis of I-V and P-V curves with uncertainty bands reveals a clear performance hierarchy: the bare reference cell performs best ($P_{max} \approx 79.6$ mW), followed by the green lens ($P_{max} \approx 71.1$ mW), the blue lens ($P_{max} \approx 65.7$ mW), and finally the reference cell with an added blue lens ($P_{max} \approx 72.4$ mW).

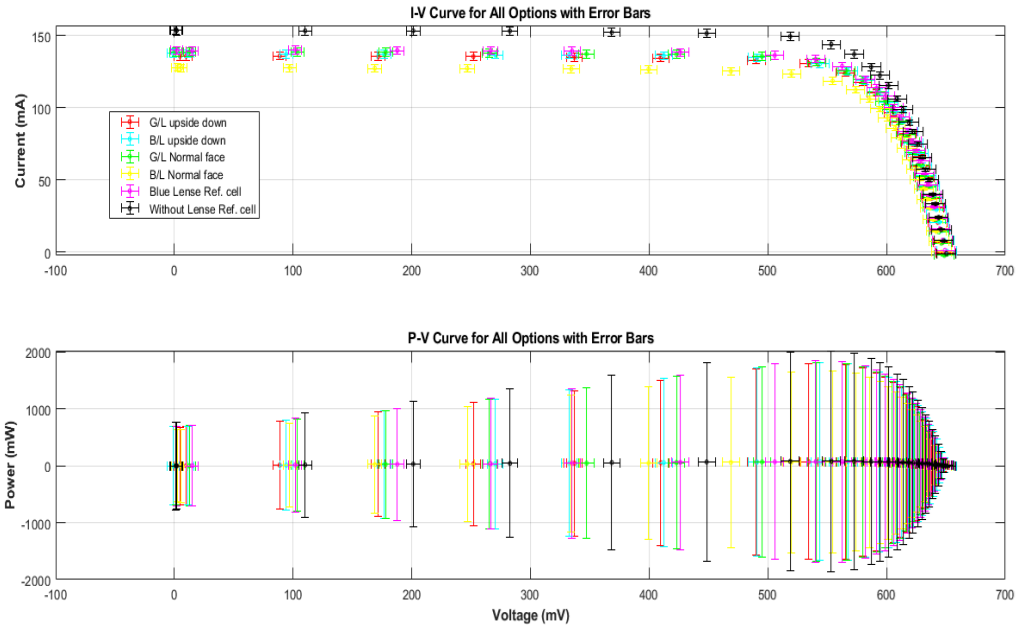

Figure 11: I-V curves and P-V curves for all options with error Bars

This trend, consistent across both current and power outputs, indicates that the green lens provides superior spectral matching to the solar cell's quantum efficiency, while the blue lens introduces greater parasitic optical losses. The narrow and consistent uncertainty bands, particularly in the current saturation region, confirm high measurement precision and lend credibility to the observed performance differences. The nearly identical open-circuit voltages across all configurations suggest the filters primarily affect photocurrent generation rather than the electronic properties of the semiconductor junction.

Figure 12: I-V curves and P-V curves for normal face and reference cell with uncertainty bands. The comparative analysis of I-V and P-V curves with uncertainty bands reveals a clear performance hierarchy: the bare reference cell performs best ($P_{max} \approx 79.6$ mW), followed by the green lens ($P_{max} \approx 71.1$ mW), the blue lens ($P_{max} \approx 65.7$ mW), and finally the reference cell with an added blue lens ($P_{max} \approx 72.4$ mW). This trend, consistent across both current and power outputs, indicates that the green lens provides superior spectral matching to the solar cell's quantum efficiency, while the blue lens introduces greater parasitic optical losses. The narrow and consistent uncertainty bands, particularly in the current saturation region, confirm high measurement precision and lend credibility to the observed performance differences. The nearly identical open-circuit voltages across all configurations suggest the filters primarily affect photocurrent generation rather than the electronic properties of the semiconductor junction.

Figure 13: I-V curves and P-V curves for upside down with uncertainty bands. The I-V and P-V curves with uncertainty bands reveal that the solar cells with green and blue lenses mounted upside down exhibit nearly identical performance, with the blue lens producing a marginally higher short-circuit current (~138 mA vs. ~136 mA) but both achieving an identical maximum power output of approximately 71 mW.

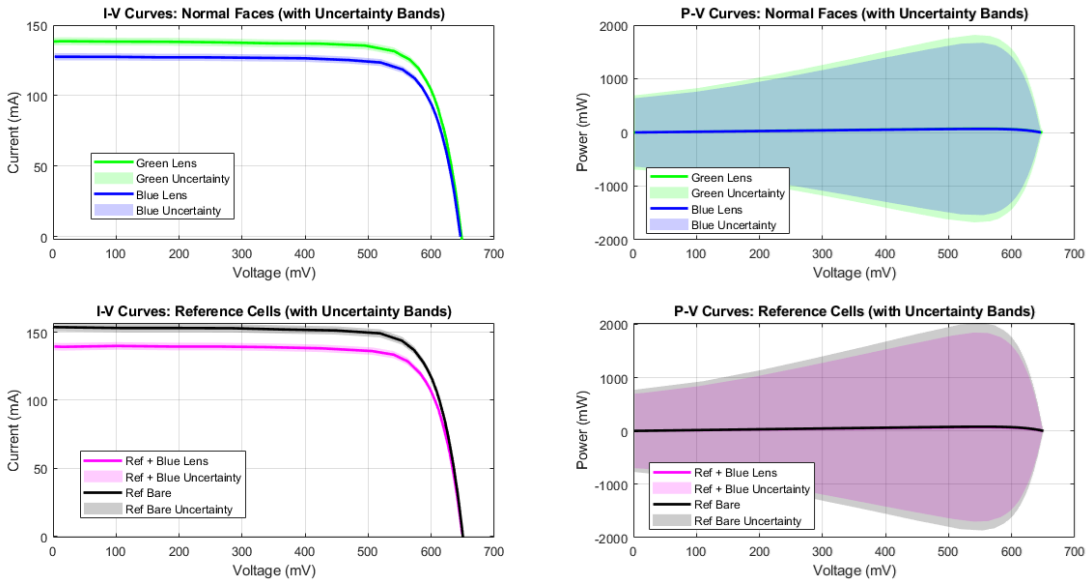

Figure 12: I-V curves and P-V curves for normal face and reference cell with uncertainty bands.

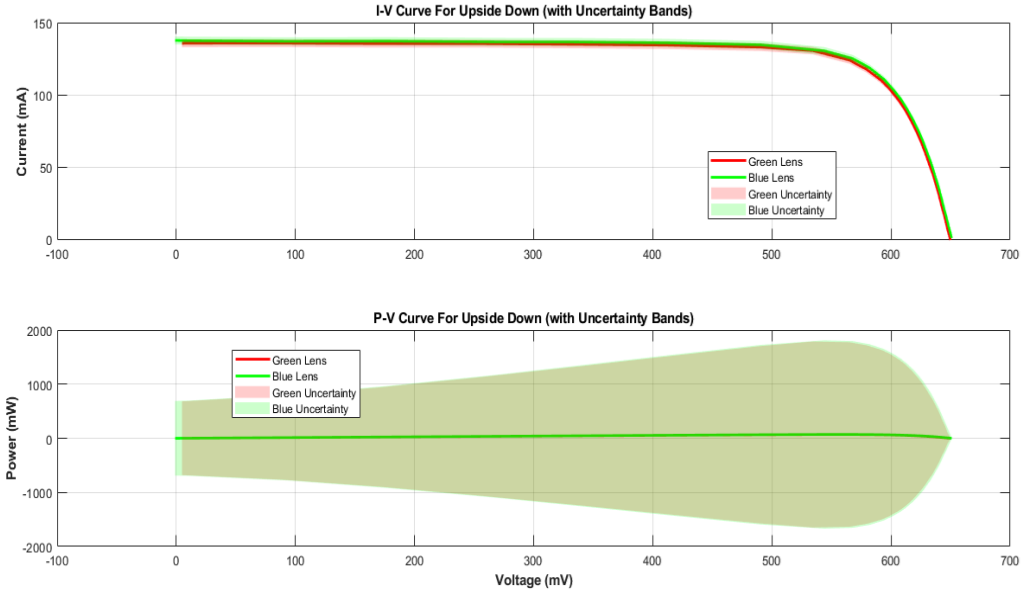

Figure 13: I-V curves and P-V curves for upside down with uncertainty bands.

The narrow uncertainty bands, particularly in the current-saturation region, indicate high measurement precision and suggest that the minimal performance difference is likely not statistically significant. This performance equivalence implies that the specific spectral filtering of the green and blue lenses has a negligible impact on power generation under these test conditions, potentially due to the "upside down" mounting configuration compromising their intended spectral selectivity or the solar cell's broad spectral response. Consequently, the data demonstrates that both lens configurations are functionally equivalent for power generation in this specific experimental setup.

5. CONCLUSIONS

In conclusion, this experimental investigation demonstrates that while the orientation of a protective lens is a critical factor significantly impacting photovoltaic performance with a reversed position causing substantial losses in short-circuit current and maximum power due

to improper light absorption, a properly aligned lens has a negligible effect compared to an uncovered cell. Furthermore, the specific lens material also plays a secondary role, as evidenced by the superior performance of the 201 LUXE (green) lens over the Blue Cut (blue) lens, which is credited to better spectral matching and lower dependent optical losses. The consistent open-circuit voltage across all tests confirms that the performance variations are primarily visual in nature, affecting photocurrent generation rather than the cell's electronic properties. These findings provide critical guidance for the solar industry, underscoring that correct installation and the selection of lenses with favorable transmission characteristics are principal for developing efficient and durable PV systems without compromising their energy output. The measured uncertainty was found to be approximately ±0.5% in voltage and ±2% in current. Future work should focus on conducting spectral response analysis to precisely quantify the wavelength-dependent losses of each lens, complemented by long-term accelerated UV testing to evaluate their durability and protective efficacy over time.

Author Contributions: Mohamed Musbah Albarghot made the initial ideas and designing the experimental work and helping with writing first draft.
Khayri Zaid made initial ideas and designing the experimental work and bought the material.
Khalifa B. Alrbee reviewed the paper in terms of writing and editing.
Mohamed A. Eltayef helped with the experimental procedure and made it ready for all the testes.
Funding source: There is no funding for the article.
Data Availability Statement: all data are available upon request.
Conflicts of Interest: The authors declare that they have no conflict of interest.
AI- Declaration: the Authors have used an AI for refences and some editing Paragraphs.
Declaration Statement: In preparation of this manuscript, Authors used (name of tool) to (type of use). Authors have reviewed and edited the manuscript and have full responsibility of the manuscript content.

REFERENCES

[1] *M. Abdunnabi, A. Abusalama, M. Algamil, and M. Almontaser, "Flat Plate based-Solar System with a tracking system Solar Energy And Sustainable Development Refereed, biannual scientific journal issued by Center for Solar Energy Research and Studies," Sol. Energy Sustain. Dev., no. 7, 2018.*

[2] *A. Elbaz, M. Bashiri, A. Almorabet, N. Elhatmi, F. Zreeq, and T. Elbouashi, "Evaluation of Power Quality in a 62.4 kW PV Grid-Connected System in Libya," Sol. Energy Sustain. Dev. J., vol. 14, no. 1, pp. 540–550, Jul. 2025.*

[3] *Y. Kombate, K. N'wuitcha, K. G. Apedanou, Y. Kolani, K. D. D. Aoukou, and B. Obese, "Analysis of Cooling Methods to Improve the Electrical Performance of Photovoltaic Modules," Sol. Energy Sustain. Dev. J., vol. 14, no. 1, pp. 410–447, May 2025.*

[4] *H. Korichi, A. Boucheham, A. B. Bensdira, and M. Kazerane, "Advancements in Passivation and Metallization Techniques for n-Type Monocrystalline Silicon Solar Cells," Sol. Energy Sustain. Dev. J., vol. 13, no. 2, pp. 151–173, Aug. 2024.*

[5] *A. Sinha et al., "UV-induced degradation of high-efficiency silicon PV modules with different cell architectures," Prog. Photovoltaics Res. Appl., vol. 31, no. 1, pp. 36–51, 2023.*

[6] *J. Fleury et al., "Electrochromic device with hierarchical metal mesh electrodes: Transmittance switching in the full spectral range of solar radiation," Sol. Energy Mater. Sol. Cells, vol. 257, no. December 2022, p. 112345, 2023.*

[7] W. Janisiewicz, F. Takeda, B. Evans, and M. Camp, "Potential of far ultraviolet (UV) 222 nm light for management of strawberry fungal pathogens," Crop Prot., vol. 150, no. August, p. 105791, 2021.

[8] D. E. King, F. J. Pern, J. R. Pitts, C. E. Bingham, and A. W. Czanderna, "Optical changes in cerium-containing glass as a result of accelerated exposure testing," Conf. Rec. IEEE Photovolt. Spec. Conf., pp. 1117–1120, 1997.

[9] L. Dunn, M. Gostein, and B. Stueve, "Literature Review of the Effects of UV Exposure on PV Modules," NREL PV Modul. Reliab. Work., vol. 16, no. February, pp. 1–19, 2013.

[10] B. L. Allsopp et al., "Towards improved cover glasses for photovoltaic devices," Prog. Photovoltaics Res. Appl., vol. 28, no. 11, pp. 1187–1206, 2020.

[11] J. B. Patel et al., "Effect of Ultraviolet Radiation on Organic Photovoltaic Materials and Devices," ACS Appl. Mater. Interfaces, vol. 11, no. 24, pp. 21543–21551, 2019.

[12] G. Perrakis, A. C. Tasolamprou, G. Kenanakis, E. N. Economou, S. Tzortzakis, and M. Kafesaki, "Ultraviolet radiation impact on the efficiency of crystalline siliconbased photovoltaics," Int. Conf. Metamaterials, Photonic Cryst. Plasmon., pp. 1080–1083, 2021.

[13] T. D. Sahlstrom, P. E. Hausgen, J. Guerrero, A. D. Howard, and N. A. Snyder, "Ultraviolet degradation testing of space protective coatings for photovoltaic cells," Conf. Rec. IEEE Photovolt. Spec. Conf., 2008.

[14] M. Tayyib, J. O. Odden, and T. O. Saetre, "UV-induced degradation study of multicrystalline silicon solar cells made from different silicon materials," Energy Procedia, vol. 38, pp. 626–635, 2013.

[15] Q. Liao et al., "Highly Stable Organic Solar Cells Based on an Ultraviolet-Resistant Cathode Interfacial Layer," CCS Chem., vol. 4, no. 3, pp. 938–948, 2022.